

Hyperbranched Polymers Analogous to PAMAM Dendrimers for the Formation and Stabilization of Gold Nanoparticles

Nelly Pérignon, Jean-Daniel Marty,* Anne-Françoise Mingotaud, Matthieu Dumont, Isabelle Rico-Lattes, and Christophe Mingotaud

Laboratoire des Interactions Moléculaires et Réactivité Chimique et Photochimique (IMRCP), UMR CNRS 5623, Université Paul Sabatier, 31062 Toulouse Cedex 09, France

Received January 23, 2007; Revised Manuscript Received February 27, 2007

ABSTRACT: Hyperbranched polymers chemically analogous to PAMAM dendrimers and their gluconamide derivatives were synthesized, and their use for gold nanoparticle synthesis and stabilization is reported. This was achieved by a two-step process: complexation of metal ions within the polymers then chemical reduction. The effect of pH values, polymer concentration, and reduction conditions on the formation and the stabilization of nanoparticles has been evaluated. Furthermore, when compared to PAMAM dendrimers, these experiments clearly demonstrated the influence of the macromolecular architecture on the formation of the metal nanoparticles.

Introduction

Metal nanoparticles have unique optical, electronic, and catalytic properties related to their small size.¹ Within the broad range of technological applications of these nanoobjects, those related to the bioanalytical and biomedical fields appear to be the most promising ones.² It then requires high stability and solubility in aqueous media combined with controllable chemical or biochemical reactivity. However, the water-based synthesis of nanoparticles is limited by inherent problems such as ionic interactions, low reactant concentration, and difficulty in removing the residue of stabilizers after synthesis. While a number of promising preparative approaches to stable, water-soluble metallic nanoparticles have been developed, few of these, if any, lead to materials that are comparable to the well-described nonpolar species in terms of stability and chemical versatility.

To overcome these problems, various molecular systems have been reported to stabilize metal nanoparticles in aqueous media, such as citrate,³ polyelectrolytes¹ or block copolymers.^{4–10} Dendrimers have been used as nanoreactors in which metal cations are localized due to complexation of the metal cations with amine groups before reduction leading to stabilized metal nanoparticles of few nanometers, this small size being presumably related to the dendrimer structure.^{11–14} They have also been used to stabilize and control the growth of nanoclusters by forming interdendrimer complexes, resulting in larger metal nanoclusters protected by the exterior amine groups of dendrimers.¹⁴ In contrast to those perfectly branched monodisperse dendrimers, randomly branched (i.e., hyperbranched) polymers can be easily accessible,¹⁵ and they can effectively stabilize metal nanoparticles in organic solvents.^{16–22}

In a previous article, we have reported a simple protocol to prepare dendritic core–shell architectures based on hyperbranched poly(ethylenimine) (PEI) with carbohydrate shells. Those compounds were used to elaborate metal nanoparticles (i.e., Cu, Ag, Au, and Pt) in water with an increased stability thanks to the carbohydrate shells.²³ In the case of platinum, catalytic activity of the corresponding nanoparticles was evidenced.²³ Preliminary reports on hyperbranched polymer

chemically analogous to PAMAM4 and with close molar mass have also shown the interesting properties of these compounds.²⁴

In the present work, we compare the complexation properties of PAMAM dendrimers to the chemically analogous hyperbranched HYPAM polymers for various molar masses and ending groups. Synthesis and characterization of a hyperbranched polymer (denoted as HYPAM5) close to PAMAM5 dendrimer as well as gluconamide persubstituted derivatives (denoted as HYPAM5G or PAMAM_xG for $x = 4$ or 5) were performed to reach such a goal. Then, gold nanoparticles preparation in water solution using these polymers as stabilizers are reported. The effect of various parameters on the formation and the stabilization of nanoparticles has been evaluated.

Experimental Section

Materials. D-Glucono-1,5-lactone, sodium borohydride (NaBH₄), hydrogen tetrachloroaurate(III) trihydrate, copper sulfate hexahydrate, and solvents were purchased from Aldrich. Tris(2-aminoethyl)amine (Aldrich) was distilled under reduced pressure and stored under argon atmosphere before use. Tris(2-di(methyl acrylate)-aminoethyl)amine (MA6-TREN) was synthesized according to the method of Dvornic.²⁵ ¹H and ¹³C NMR data were in accordance with the literature.^{26,27} PAMAM4 and PAMAM5 dendrimers (respectively fourth and fifth generations) as well as PAMAM4OH (dendrimer of the fourth generation bearing 64 surface hydroxyl groups) were purchased from Aldrich and used without further purification.

Characterization. ¹H NMR spectra were recorded on a Bruker AC 250 spectrometer at 250.13 MHz and on a Bruker ARX 400 at 400.13 MHz. ¹³C NMR spectra were recorded on a Bruker Avance 300 spectrometer at 75.47 MHz and on a Bruker ARX 400 at 100.61 MHz. Attribution of the signals was made by COSY, HSQC and HMBC experiments and comparison with corresponding spectra of PAMAM dendrimers. Quantitative ¹⁵N NMR was carried out on a Bruker AMX400 at 40.55 MHz with a delay between pulses of 100 s (probe head for 10 mm tubes, 30° pulse of 20 μs, inverse-gated proton-decoupled experiments). Quantitative ¹³C NMR was carried out with a delay between pulses of 55 s. The quantitative response was checked with a test solution of known concentrations of Me₄NOH and ethylenediamine.

The average molecular weight of the polymers was determined by size exclusion chromatography (SEC) analysis in carbonate buffer solution at pH 10 (flow rate 0.5 mL/min) on an apparatus equipped with a Waters refractive index detector, a Waters column

* Corresponding author: E-mail: marty@chimie.ups-tlse.fr. Telephone: 33 561-556-135. Fax number: 33 561-558-155.

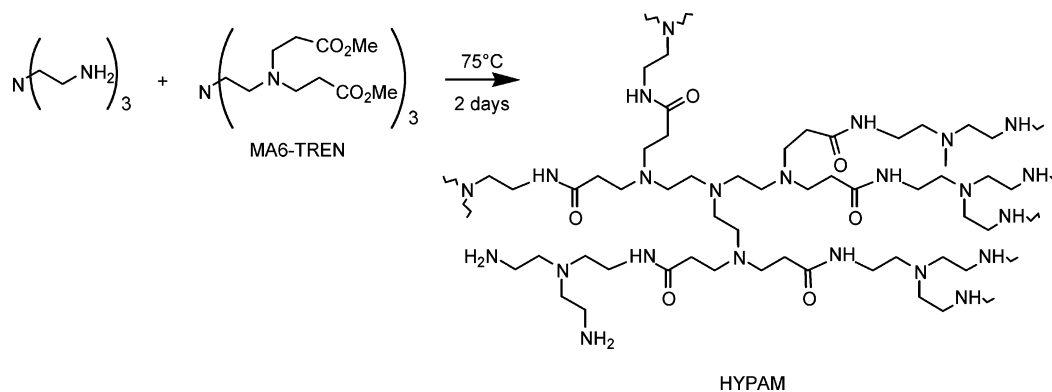


Figure 1. Schematic representation of the synthesis and structure of the HYPAM hyperbranched polymer.

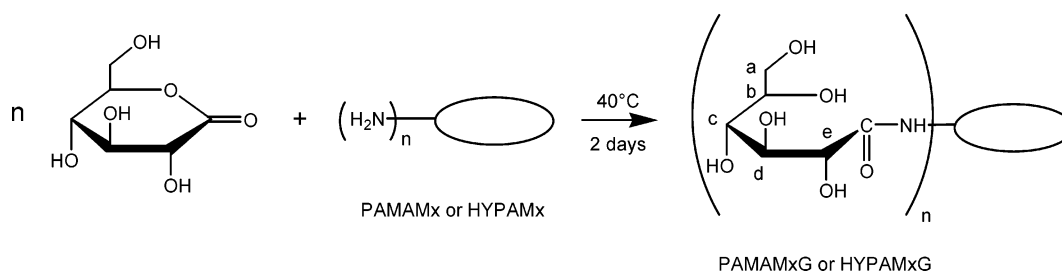


Figure 2. Functionalization of PAMAMx and HYPAMx by gluconolactone to lead to PAMAMxG and HYPAMxG.

pack (Shodex OHPak SB-802HQ, SB-802.5HQ, SB-804HQ) and a Minidawn Wyatt light scattering detector. The molecular weights were uncorrected from low sensitivity of LS-SEC to lower molecular weights.²⁸ The refractive index increments for PAMAM dendrimers were measured in the same eluent at ambient temperature. The values for the hyperbranched polyamides were assumed to be identical. Considering the fact that these polymers have been observed to trap solvent molecules, even after prolonged drying under vacuum, the accuracy for the molecular weight measurement is estimated to be around 20%.

UV-visible spectra of solutions were recorded with a HP 8452A diode array spectrometer (optical pathlength: 0.5 cm).

Transmission electron microscopy (TEM) was performed on a Hitachi HU12A transmission electron microscope operating at 125 kV accelerating voltage. To prepare samples for analysis, an aqueous solution of coated nanoparticles was drop-cast onto carbon-coated copper TEM grids (Formvar support, 300 mesh, Ted Pella Inc.).

Preparation of Hyperbranched Polyamidoamines (Figure 1). The hyperbranched polymers were prepared according to the method of Dvornic. Synthesis of the HYPAM4 has been already described.²⁴ For HYPAM5, 2.44 g of tris(2-aminoethyl)amine (16.7 mmol) were mixed with 1.42 g of MA6-TREN (2.14 mmol). The solution was stirred under argon at 70 °C during 2 days, after which the products were dissolved in 5 mL of CH_2Cl_2 and precipitated into 200 mL of THF at 0 °C. Thus, 2.37 g of precipitated polymer was obtained as a yellow gum. ^1H NMR (CDCl_3 , 250.13 MHz): 2.1–2.9 (m, NH_2 , $-\text{CH}_2-\text{NH}_2$, $-\text{CH}_2-\text{CO}-$); 3.25 (br m, $-\text{CH}_2-\text{NHCO}-$); 8.29 (br s, $-\text{NHCO}-$). ^1H NMR (D_2O , 400.13 MHz): 2.34 (m, $-\text{CH}_2-\text{CO}-$); 2.5 (m, $\text{N}-\text{CH}_2-\text{CH}_2-\text{N}$); 2.55 (m, $\text{CONH}-\text{CH}_2-\text{CH}_2-\text{N}$); 2.63 (m, $-\text{CH}_2-\text{NH}_2$); 2.73 (m, $\text{N}-\text{CH}_2-\text{CH}_2-\text{CO}$); 3.22 (m, $-\text{CH}_2-\text{NHCO}-$). ^{13}C NMR (D_2O , 75.47 MHz): 32.6 35.5 ($-\text{CH}_2-\text{CO}$); 36.7 ($-\text{CH}_2-\text{NH}-\text{CO}-$); 37.8 ($-\text{CH}_2-\text{NH}_2$); 49.1 ($\text{N}-\text{CH}_2-\text{CH}_2-\text{CO}$); 49.8 51.1 52.5 ($\text{CONH}-\text{CH}_2-\text{CH}_2-\text{N}$); 56.0 ($\text{N}-\text{CH}_2-\text{CH}_2-\text{N}$); 174.5 (CONH).

Preparation of Gluconamide-Polyamides (Figure 2). For the synthesis of PAMAMxG ($x = 4$ or 5), the grafting of gluconolactone was carried out according to an already published procedure.²⁹ For HYPAM5G, a solution of 0.85 g of HYPAM5 (4.7 mmol of primary amine groups), 1.7 g of gluconolactone (9.5 mmol), and 5 mL of dry DMSO was stirred at 40 °C during 48 h under argon. The

polymer was precipitated into 150 mL of MeOH and recovered by centrifugation at 14500 rpm during 30 min at 5 °C. 1.0 g of modified polymer was obtained. ^1H NMR (D_2O , 400.13 MHz): 2.40 (m, $-\text{CH}_2-\text{CO}-$); 2.68 (m, $\text{N}-\text{CH}_2-\text{CH}_2-\text{N}$); 2.80 (m, $\text{N}-\text{CH}_2-\text{CH}_2-\text{CO}$); 3.23 (m, $-\text{CH}_2-\text{NHCO}-$ polyamide); 3.29 (3, $-\text{CH}_2-\text{NHCO}-$ gluconamide); 3.59 and 3.75 (ABX system $J = 11$ Hz, $-\text{CH}_2\text{OH}$); 3.66 (m, $-\text{CHOH}-b$ and $-c$); 4.01 (m, $-\text{CHOH}-d$); 4.23 (m, $-\text{CHOH}-e$). ^{13}C NMR (D_2O , 75.47 MHz): 32.7 ($-\text{CH}_2-\text{CO}$); 36.7 ($-\text{CH}_2-\text{NH}-\text{CO}-$ gluconamide); 37.1 ($-\text{CH}_2-\text{NH}-\text{CO}-$ polyamide); 49.3 ($\text{N}-\text{CH}_2-\text{CH}_2-\text{CO}$); 52.4 ($\text{N}-\text{CH}_2-\text{CH}_2-\text{N}$); 62.8 ($-\text{CH}_2\text{OH}$); 70.5 ($-\text{CHOH}-d$); 71.3 ($-\text{CHOH}-b$); 72.4 ($-\text{CHOH}-c$); 73.6 ($-\text{CHOH}-e$); 174.5 (CONH). (see Figure 2 for NMR attribution).

Typical Procedure for Complexation Studies. An aqueous solution of the respective stabilizer (concentrations calculated with the \overline{M}_w value) was mixed with an aqueous solution of metal ion (CuSO_4 , HAuCl_4) in order to obtain a determined molar ratio [metal ion]/[polymers] (in the range 10–300). Absorbance spectra were recorded after 48 h.

Formation of Nanoparticles. Typically, a determined amount of CuSO_4 or HAuCl_4 was dissolved in a 5.10^{-6} M aqueous solution of the stabilizer to obtain the appropriate [metal]/[stabilizer] ratio. Complexes were then chemically reduced with various molar excess of NaBH_4 (1, 5, 11, 16, ...) respective to the metal ions to yield zerovalent metal particles.

Results and Discussion

1. Synthesis of Hyperbranched Polyamidoamines. The synthesis of hyperbranched polymers with a similar structure as PAMAM dendrimers was based on a method described by Dvornic, where a hexaester is reacted with a triamine (Figure 1).²⁵ This method has the advantage to lead to the hyperbranched structure in a single step and can be carried out in large quantities. Its main drawback is to give polymers with broad distributions. The molecular weight of the polymers was easily adjusted by changing the ratio between the triamine and the hexaester (MA6-TREN). For a 10:1 molar ratio, it is close to the one of a PAMAM of the fourth generation.²⁴ This hyperbranched polymer was therefore noted HYPAM4. A ratio close

Table 1. Properties of Investigated Polymers

	\overline{M}_w^a	$I = \overline{M}_w/\overline{M}_n^b$	primary amines/tertiary amines/amide groups (mmol.g ⁻¹)
PAMAM4 ^c	13000 (14215) ^d	1.1	3.8/3.9/7.1 ^e (4.5/4.4/8.7) ^d
PAMAM4G	27700 (25615) ^d	1.3	0/3.9/10.9 ^f (0/2.4/7.3) ^d
PAMAM4OH	n.d. (14279) ^d		n.d. (0/4.3/8.7) ^d
HYPAM4 ^c	13 600	1.4	4.9/5.0/3.3 ^e
PAMAM5	n.d. (28825) ^d		n.d. (4.4/4.4/8.7) ^d
PAMAM5G	n.d. (51627) ^d		n.d. (0/2.4/7.4) ^d
HYPAM5	30 300	2.2	5.5/5.1/3.7 ^e
HYPAM5G	116200 (60000) ^f	4.7	0/2.6/4.6 ^f

^a Molecular weight determined by LS-SEC. ^b Polydispersity index determined by SEC. ^c Values extracted from ref 24. ^d Theoretical values deduced from the ideal chemical structure. ^e Results obtained from quantitative ¹³C NMR experiments. ^f Deduced from the characterization of the corresponding nonglycosylated compounds.

to 8:1 led to a polymer noted HYPAM5 (see Experimental Section), its molar mass being close to the one of PAMAM5. Those molar masses were evaluated by size exclusion chromatography (SEC) in carbonate buffer at pH 10 equipped with a refractive index detector and a light scattering detector. A typical chromatogram is presented in supporting data and all the results are given in Table 1. The attachment of D-glucono-1,5-lactone to HYPAMx was carried out according to an already published procedure with PAMAM dendrimers.²⁹ Primary amino groups were quantitatively functionalized as demonstrated by ¹H NMR.

The analysis of hyperbranched polymers by SEC has been the subject of many articles.^{28,30–32} Because of the singular architecture, a regular analysis with standard calibration is not valid. The use of light scattering detector together with a refractometric one, provides an evaluation of the molecular weight of the polymers. However, even with this approach, for wide distributions, the difference of sensitivity of light scattering between high and low molecular masses leads to an underestimated polydispersity index. Some authors have proposed a method to compensate for this effect.²⁸ In our case, this correction led to an increase of the polydispersity index only for HYPAM5 and HYPAM5G samples (respectively from 2.2 to 4.9 and from 4.7 to 6.8). However, if the use of this program is relevant for regular linear polymers, it might not be in our case, since some interactions between the polymer and the column might still be present besides size exclusion. Therefore, the molar masses and polydispersity indices presented in Table 1 are not corrected. Furthermore, these polymers (as well as PAMAM dendrimers) have been observed to trap solvent molecules even after prolonged drying. Thus, the measured molecular weights should be considered as indicative values. For the PAMAM dendrimers, the SEC analysis were consistent with the expected values. For sugar-modified polymers, the strong increase in molecular weight compared to the theoretical value was likely related to an aggregation phenomenon, even in aqueous buffer solution. This was particularly strong for HYPAM5G.

In order to compare the structure of the HYPAM hyperbranched polymers with the one of PAMAM dendrimers, titration of the amine groups for the polymers was also carried out by several methods: simple acid–base titration,^{33–35} quantitative ¹⁵N NMR^{34,36} and quantitative ¹³C NMR. While titration for well-defined dendrimers has been analyzed, the titration steps for the hyperbranched polymers presented here were, in certain cases, too unclear to be unequivocally attributed. As for ¹⁵N NMR, the titration was tested by introducing a calibration product in the NMR tube. With appropriate relaxation

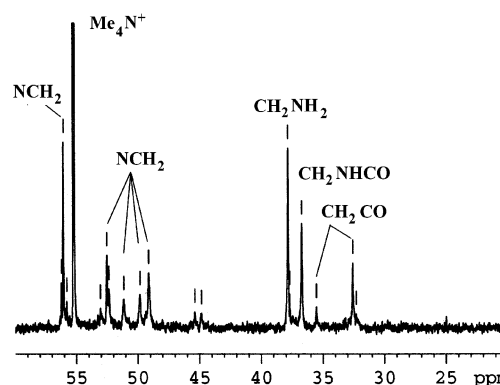


Figure 3. ¹³C NMR spectrum of HYPAM5 used for the quantitative titration within the polymer of primary amine groups (CH₂NH₂), tertiary amine groups (NCH₂) or amide groups (reference: Me₄N⁺ peak).

times, the quantitative determination of primary amine groups was possible. However, the quantity of polymer needed for this experiment (more than 0.8 g per tube) as well as the time needed (60 h) incited us to abandon this method. Best results were then obtained by quantitative ¹³C NMR experiments in the presence of a calibration product (Me₄NOH). A typical spectrum is reported in Figure 3.

The attribution of the peaks was carried out by COSY, HSQC, and HMBG experiments and comparison with corresponding spectra of PAMAM dendrimers. Comparison of the CH₂–NH₂ peak at 37.8 ppm to Me₄NOH peak at 55.2 ppm led to an evaluation of the quantity of primary amine groups. For PAMAM4, this method gave a value of 3.8 mmol per gram, which is relatively close to the theoretical one (4.5 mmol per gram).²⁴ Table 1 shows that the quantity of primary amine groups was found slightly higher for the other polymers used in this study.

Comparing HYPAM and PAMAM polymers at more or less constant molecular weight (i.e., HYPAM4(G) with PAMAM4-(G) and HYPAM5(G) with PAMAM5(G)), the number of primary and tertiary amines were close regardless of the structure (see Table 1). The largest difference between those two types of polymers was the quantity of amide groups within the polymer: by construction, these values are largely reduced in the hyperbranched structure compared to dendrimers.

Polymer-stabilized nanoparticles were prepared in a two-step process. Initially, an aqueous solution of the polymer (at various concentrations) was mixed with an aqueous solution of metal ions (CuSO₄, HAuCl₄) to obtain a controlled molar ratio [metal ions]/[polymer]. In a second step, the ions were chemically reduced by sodium borohydride (with different molar excess of metal ions varying from 1 to 10). While the conditions for the reduction are paramount for the final stability of the nanoparticles, the interactions metal ions/polymer should be understood in order to control the size of the metal clusters. Complexation properties of the dendritic architectures were therefore studied with copper and gold ions.

2. Complexation with Metal Cations. For these experiments, solutions were equilibrated during 1 h or more before measurements. All solutions had a pH around 4. As pK_{NH2} value in HYPAM_x should be close to the one estimated for NH₂ functions in PAMAM₄, i.e., 9.5,³³ HYPAM_x could be assumed mainly in the protonated form under those conditions.

In the case of copper, complexation occurred on a time scale shorter than a minute. Figure 4 reports the UV–visible spectra of Cu(II) solution with or without HYPAM5G. In aqueous solutions and without any polymer, Cu^{II} exists primarily as [Cu(H₂O)₆]²⁺, which gives rise to a broad and weak absorption

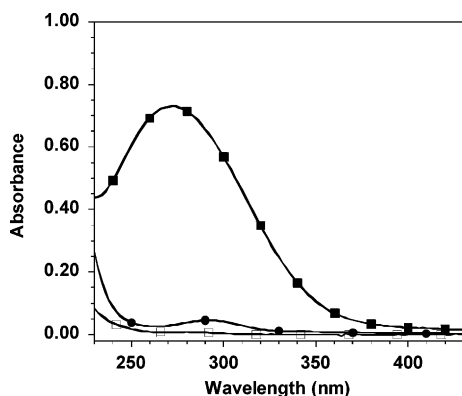


Figure 4. Absorption spectra of aqueous solutions: 6×10^{-4} M CuSO_4 (open squares), 3.10×10^{-6} M of HYPAM5G (full circles), 6×10^{-4} M CuSO_4 and 3×10^{-6} M of HYPAM5G (full squares).

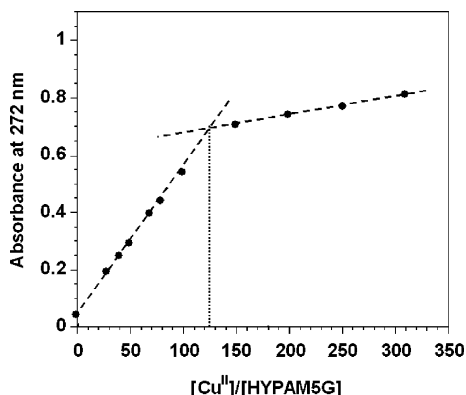


Figure 5. Absorbance at 272 nm of a solution 3×10^{-6} M of HYPAM5G with various amount of Cu^{II} .

band at ca. 810 nm associated with a d–d transition ($\epsilon \sim 10$) (not shown).¹² In the presence of the hyperbranched polymer, the Cu^{II} d–d transition shifted to 605 nm ($\epsilon \sim 30$).²⁴ In addition to those weak bands, a strong ligand-to-metal charge-transfer (LMCT) transition appeared at ca. 270 nm (see Figure 4): this new band as well as the shifted d–d transition suggested interactions and/or complexations between the metal ions and the polymers (presumably through the amine and amide groups³⁷). The change in the UV–visible spectrum depending on the $[\text{Cu}^{\text{II}}]/[\text{polymer}]$ molar ratio allowed us to follow this complexation process. Indeed, the absorbance at the maximum (i.e., 272 nm) of this new band increased with the $[\text{Cu}^{\text{II}}]/[\text{polymer}]$ ratio (see Figure 5). Initially, the increase was linear with the molar ratio, suggesting a progressive loading of the polymer by copper ions. Then, a large decrease in the slope of the curve was recorded and was assigned to the saturation of the hyperbranched structure. HYPAM polymers have therefore a behavior quite similar to that of PAMAM dendrimers.¹² An estimation of the titration end point was obtained by extrapolating the two linear regions of the previous curve (see Figure 5), indicating that HYPAM5G can complex up to 130 Cu^{II} ions (see Supporting Information for complexation data of HYPAM4 and HYPAM5 with copper).

In the case of $\text{Au}(\text{III})$, slow kinetics have been reported for complexation with dendrimers.³⁸ To avoid any problems, the incubation time for gold uptake was chosen to be equal to 48 h, although due to the lower degree of branching, complexation with hyperbranched polymers should occur more rapidly (no significant evolution of the spectra was observed 24 h after the beginning of the complexation process). All samples were stable on this time scale if protected from light exposure. As already described in a previous article,²⁴ the absorption spectrum of an

Table 2. Complexation Properties of PAMAMx and HYPAMx

polymer	maximum load of ions		no. of functional amines (primary/tertiary/amides)
	CuSO_4	HAuCl_4	
PAMAM4 ^a	46 ± 5	47 ± 5	64/62/124
PAMAM4G	40 ± 5	52 ± 5	0/62/188
PAMAM4OH	24 ± 5	20 ± 5	0/62/124
PAMAM5	85 ± 10	N.D.	128/126/252
HYPAM4 ^a	90 ± 10	150 ± 10	67/68/45
HYPAM5	135 ± 10	180 ± 10	167/155/112
HYPAM5G	130 ± 10	160 ± 10	0/155/279

^a Extracted from ref 24.

aqueous HAuCl_4 solution exhibited a strong absorption band at 226 nm and a shoulder at 290 nm due to charge transfer between the metal and the chloro ligands beside a very weak band around 640 nm. When adding the hyperbranched polymer, the absorbance at 290 nm increased linearly with the number of added metal ions until a particular $[\text{metal ion}]/[\text{polymer}]$ ratio. Above this ratio, a change in slope was observed (see ref 24 and Supporting Information for complexation data with the various polymers). The difference in slopes suggested different surroundings for the added gold ions and therefore some interactions between gold ions and the polymer. The nature of interactions was not yet fully determined, but as already described in the case of chitosan,³⁹ considering that HAuCl_4 has a $\text{p}K_{\text{a}}$ lower than 3, formation of ion pairs between AuCl_4^- and the protonated amino groups of HYPAMx (the $\text{p}K_{\text{NH}_2}$ value in HYPAMx was estimated to 9.5²⁴) could be responsible at least partially for this phenomenon. Nevertheless, in the case of HYPAM4, this limit ratio (150) was larger than the primary amine functions of HYPAM4 (ca. 70 as deduced from Table 1) and close to the number of amine and amide functions within the polymer (estimated to ca. 180), suggesting more complex interactions between gold ions and polymers.

Because of differences in the mechanism of interactions, copper ions led to smaller maximum loading values than those for the gold ions. The critical ratio associated with the saturation of the polymer was strongly related to the type of polymer used (see Table 2). The primary structure (dendrimer against hyperbranched polymer) was clearly one of the most important parameter controlling the maximum loading of the polymer. Whereas the maximum number of loaded metal ions for PAMAM4 was found around 50, HYPAM4 had a maximum load of copper or gold metal cations equal respectively to 90 and 150. The open structure of the hyperbranched polymer compared to the dendrimer architecture facilitated the interactions of the metal ions with the internal chemical functions and led therefore to an increase of the maximum load of ions per polymer. The influence of the polymer molar mass was quite similar in the case of PAMAM and HYPAM. The increase in the polymer generation induces a growth of the maximum load of metal ions, even if this increase was proportionally less pronounced in the case of HYPAM than in the case of PAMAM¹² (respectively, 25% and 50%). Finally, the substitution of NH_2 groups by gluconic amide groups did not significantly modify the complexation properties of the different systems studied, suggesting that the amide functions of the dendritic skeleton participated to the interaction between the polymers and the metal ions.

All these results show that it is possible to load the dendritic architectures to various metal levels by adding controlled quantities of metal ions on the polymer solution. These results are similar to those obtained with dendrimers for which similar properties have already been demonstrated.¹⁴

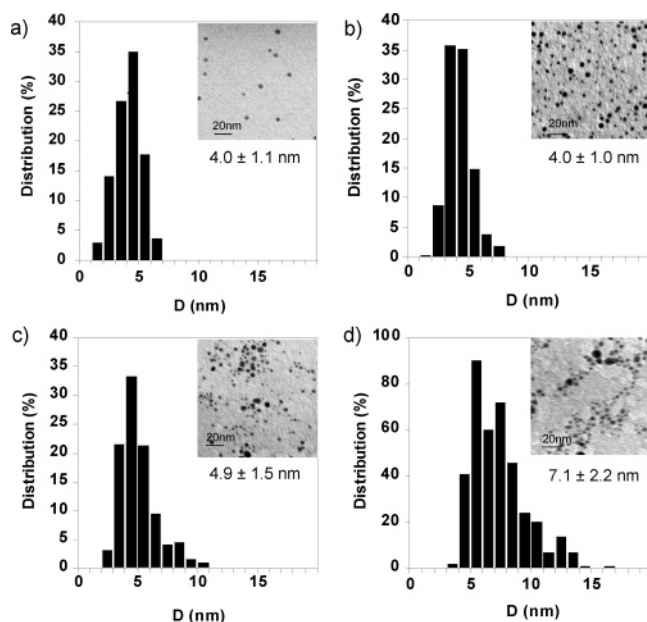


Figure 6. TEM micrographs and corresponding histograms (ca. 300 nanoparticles analyzed) illustrating the gold nanoparticles diameter (D) distribution of HYPAM4 with various ratios $[\text{HAuCl}_4]/[\text{HYPAM4}]$: (a) 60 (adapted from ref 24); (b) 120; (c) 180; (d) 240 ($[\text{NaBH}_4]/[\text{HAuCl}_4] = 5$).

3. Formation of Nanoparticles. In order to obtain the nanoparticles, reduction of the cations loaded in the polymer was carried out with a 1–50 fold excess of dissolved NaBH_4 (respective to metal ions). In all cases, an immediate color change of the solution was observed and assigned to the formation of copper and gold nanoparticles. In the case of gold complexes, the 226 nm band of AuCl_4^- vanished, indicating that the AuCl_4^- ions were completely reduced.²⁴ Instead, a broad band appeared at around 540 nm, which is assigned to a plasmon band of gold particles.²⁴ Furthermore, a very weak shoulder was observed at ca. 280 nm and may be due to some irreversible oxidation of the polymer by gold ions. In the case of copper, a plasmon band appeared at ca. 570 nm. Copper nanoparticles easily reoxidize in Cu(II) ions if not maintained under an inert atmosphere. Consequently further studies will focus on the more stable gold nanoparticles. Figure 6a shows a transmission electron microscopy (TEM) micrograph of gold nanoparticles coated with HYPAM4 (see Supporting Information for nanoparticles coated with HYPAM5 and HYPAM5G). The particles are well isolated with a low dispersity in size. The mean particle size was determined to be ca. 4 nm. Electron diffraction micrographs of these nanoparticles fitted well with expected pattern associated with gold metal.

A question arising from these first experiments is whether the growth of particles is controlled by confinement effect due to specific adsorption of hyperbranched polymers or only by the nucleation process. When comparing sizes obtained by reducing gold ions by a 5-fold excess of sodium borohydride with or without HYPAM4, it clearly appeared that nanoparticles obtained in presence of HYPAM4 were smaller (respectively 6.9 and 4.0 nm). Moreover nanoparticles without any stabilizer were not stable in these conditions (pH around 6.5) and rapidly increased in size (after 2 h size was greater than 9 nm). Therefore, the use of HYPAM allows one to control of the growth of gold nanoparticles.

Starting from these preliminary experiments, we then analyzed the influence of the reduction agent, the $[\text{polymer}]:[\text{metal}]$

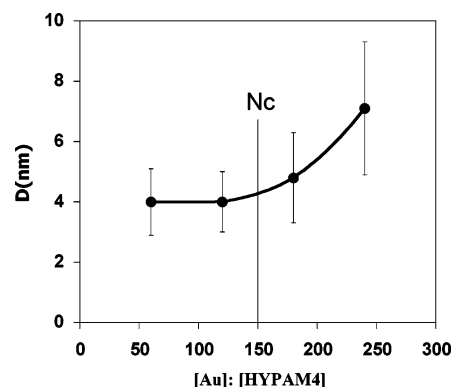


Figure 7. Mean diameter size (with standard deviation) of gold nanoparticles formed by reduction with NaBH_4 ($[\text{NaBH}_4]/[\text{HAuCl}_4] = 5$) as a function of $[\text{HAuCl}_4]/[\text{polymer}]$ ratio for HYPAM4.

ratio and the polymer architecture (composition and molar mass) on the size of the nanoparticle obtained.

3a. Influence of the Conditions of Reduction. Conditions of reduction greatly influenced the formation of nanoparticles. The reduction of gold ions with large excess of sodium borohydride induced a slight decrease in the size of nanoparticles. For instance, for HYPAM4 system, when $[\text{NaBH}_4]/[\text{HAuCl}_4]$ was increased from 1 to 5, nanoparticles were obtained with an average size of respectively 5.6 ± 1.6 nm and 4.0 ± 1.0 nm. For greater excess, this effect was difficult to control as a change in $[\text{NaBH}_4]/[\text{HAuCl}_4]$ ratio induced also a change in the pH and consecutively a modification in the stabilizer conformation. When amino groups were substituted by gluconic amide groups (HYPAMxG structure), gold ions were found to undergo reduction without adding any reducing agent but with very slow kinetics.⁴⁰ Nanoparticles obtained in that case were larger (15 nm) with a broader distribution in size and an uncontrolled morphology.

3b. Influence of the Metal:Polymer Ratio. Figure 7 represents the evolution of mean size as a function of $[\text{HAuCl}_4]/[\text{polymer}]$ for HYPAM4 for $[\text{NaBH}_4]/[\text{HAuCl}_4] = 5$. For this one, no significant difference with NaBH_4 used as reducing agent appeared in the size distribution for ratios below the maximum loading ratio (N_c). Reduced systems, with a $[\text{HAuCl}_4]/[\text{polymer}]$ ratio higher than the maximum loading ratio, induced the formation of bigger nanoparticles with larger size distribution. These systems were also observed to be less stable: e.g., after 1 day complete aggregation occurred. The growth of gold nanoparticles outside hyperbranched structure occurred more rapidly and induced a complete aggregation of gold nanoparticles by capping the formed gold particles. Thus, the interactions between the stabilizer and the gold ions before and during reduction appeared to be the key factor for the growing process. Similar results were obtained with HYPAM5 and HYPAM5G (see Table 3).

3c. Influence of the Molecular Weight of the Polymeric Core and the Substitution of Primary Amino Groups. For a low $[\text{HAuCl}_4]/[\text{polymer}]$ ratio (i.e., 60), the average particle size of gold nanoparticles increased with increasing molecular weight of the polymer (HYPAM4, $4.0 \text{ nm} \pm 1.1 \text{ nm}$; HYPAM5, $6.5 \text{ nm} \pm 2.1 \text{ nm}$), and just slightly increased by attaching gluconolactone to the amine groups (HYPAM5, $6.5 \text{ nm} \pm 2.1 \text{ nm}$; HYPAM5G, $7.7 \pm 2.7 \text{ nm}$). Moreover, for HYPAM5 or HYPAM5G, below the maximum loading ratio, there was a slight increase of mean size by increasing the $[\text{AuCl}_4]/[\text{polymer}]$ ratio (Table 3). Similarly, it was reported in the literature that a PAMAM: Au ratio of 1:10 (M_n PAMAM of generation 5.5 =

Table 3. Mean Size of Gold Nanoparticles as a Function of $[\text{HAuCl}_4]/[\text{polymer}]$ for HYPAM4, HYPAM5, and HYPAM5G^a

$[\text{Au}^{\text{III}}]/[\text{HYPAMx(G)}]$	D (nm) \pm standard deviation		
	HYPAM4	HYPAM5	HYPAM5G
60	4.0 ± 1.1^b	6.5 ± 2.1	7.7 ± 2.7
90		6.6 ± 2.2	8.3 ± 2.7
120	4.0 ± 1.0^b	7.1 ± 2.6	
180	4.9 ± 1.5		9.0 ± 2.2
240	7.1 ± 2.2^b	7.5 ± 2.3	
300			6.4 ± 3.3^c

^a Data obtained from TEM measurements after reduction by a 5-fold molar excess (relative to Au^{III}) of NaBH_4 . Drop-cast onto TEM grids was realized 1 h after reduction. ^b Extracted from ref 24. ^c Partial precipitation occurred before TEM deposition, so in this case mean size was evaluated only for the remaining nanoparticles in solution. This explains the significant decrease in size for this sample.

$50\,864\text{ g mol}^{-1}$) gave a mean particle size of 5.6 nm, whereas at a ratio of 10:1 the synthesized particles were smaller (2.3 nm).⁴¹

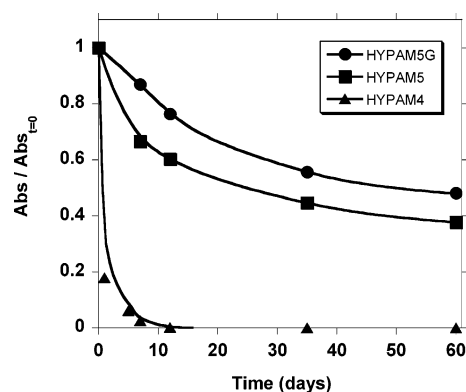
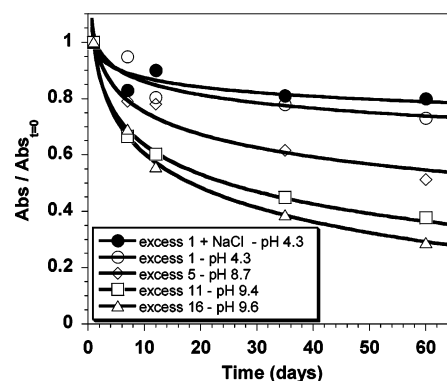
All these results led us to the following conclusions: (1) The hyperbranched HYPAM polymers enables the formation of gold nanoparticles of different sizes (below 10 nm). The size could be controlled by adjusting the $[\text{HAuCl}_4]/[\text{polymer}]$ ratio, $[\text{NaBH}_4]/[\text{HAuCl}_4]$ ratio, changing molecular weight or modifying the chemical structure of the hyperbranched polymer. (2) Most particles obtained are too large to be contained inside a single hyperbranched polymer. These particles are most likely to be capped by multiple polymer chains as has been demonstrated in the literature concerning some dendritic or hyperbranched systems.^{23,24} The well-defined architecture of dendrimers seems to be best suited to confine growth of the nanoparticles inside a single dendrimer. Nevertheless, template effect with hyperbranched polymer could be obtained by lowering $[\text{HAuCl}_4]/[\text{polymer}]$ ratio as demonstrated in hyperbranched PEI systems.²³

4. Stabilization Properties. Numerous publications deal with the stability of metal nanoparticles in relation with the $[\text{polymer}]:[\text{metal ratio}]$,^{4,5,41,42} pH of the solution,^{4,43} concentration of the polymer in solution,^{6,7,41,42} concentration of metal cations in solution⁶ and the reduction agent applied.^{4,5} Parameters that influence the stability of nanoparticles, such as the molecular weight of the polymer core, the pH of the solutions, the $[\text{polymer}]:[\text{metal}]$ ratio were investigated and are reported here.

As previously mentioned, to avoid a rapid destabilization of the hyperbranched capped nanoparticles, reduction should occur below the maximum loading ratio. In the following experiments, long-term stability was studied with the $[\text{HAuCl}_4]/[\text{polymer}]$ ratio equal to 120 for all solutions.

To estimate the stability of the nanoparticles vs time, we have monitored the UV spectra of the solution. The evolution of absorbance at 520 nm normalized by absorbance at zero time as a function of time for gold nanoparticles stabilized by HYPAM4, HYPAM5, or HYPAM5G at room temperature with $[\text{NaBH}_4]/[\text{HAuCl}_4] = 11$ is represented in Figure 8. Whereas HYPAM4 systems were stable for a relatively short period (less than a week), in contrast HYPAM5 ones were stable for months (decrease of 60% of the absorbance after 2 months). Therefore, the increase of the molecular weight improved the overall stability of the gold nanoparticles. This is probably due to the increase of the steric hindrance. Moreover, in these conditions, functionalization of amino groups with gluconolactone slightly improved the stability of gold nanoparticles.

After the molecular weight of the polymer, we were interested in the effect of the pH on the gold nanoparticle stability. The primary effect of excess borohydride was to raise the pH of the

**Figure 8.** Evolution of absorbance at 520 nm as a function of time for gold nanoparticles stabilized by HYPAM4 (full triangle), HYPAM5 (full square) or HYPAM5G (full circle) at room temperature with $[\text{NaBH}_4]/[\text{HAuCl}_4] = 11$.**Figure 9.** Evolution of absorbance at 520 nm as a function of time for gold nanoparticles stabilized by HYPAM5 formed with presence of various excess of NaBH_4 (1, 5, 11, and 16 comparative to gold ions Au^{III}) or in presence of NaBH_4 (excess 1) and NaCl (excess 10).

solution (excess 1, pH = 4.3; excess 5, pH = 8.7; excess 11, pH = 9.4; excess 16, pH = 9.6). Figure 9 shows the evolution of absorbance at 520 nm as a function of time for gold nanoparticles stabilized by HYPAM5 after addition (at $t = 0$) of various amounts of excess sodium borohydride (1, 5, 11, 16 comparative to gold ions HAuCl_4). Stability of the systems decreased when increasing the amount of NaBH_4 , i.e., when increasing pH value. To check if the effect observed was not simply the result of change in ionic strength, addition of NaCl on the solution obtained with a stoichiometric amount of NaBH_4 (pH = 4.3) up to concentrations equivalent to the addition of 11-fold excess of borohydride was performed. As shown in Figure 9, no significant change in the absorbance evolution was observed between 1 excess of NaBH_4 and 1 excess of NaBH_4 plus NaCl . So, the main factor controlling stability was the pH of the solution. This result was in good agreement with the level of protonation of amino group. At lower pH value, amino groups are mainly protonated: electrostatic repulsion improved stability of HYPAM5-stabilized gold nanoparticles. When increasing pH, amino groups were deprotonated and stability decreased. This was confirmed by measuring ζ potentials of gold-capped nanoparticles that decrease by increasing pH (supporting data).

The effect of functionalization on stability was then evaluated. HYPAM5G was clearly unaffected by pH changes due the functionalization of pH sensitive amino groups by gluconolactone.

Ionic strength was increased to study the effect of the polymer outer shell on stability. Seven HYPAM5 and HYPAM5G stabilized gold nanoparticles solutions, at pH ~ 9 , were added with increasing quantity of NaCl (from 0 to 0.1 mol L^{-1}). Their

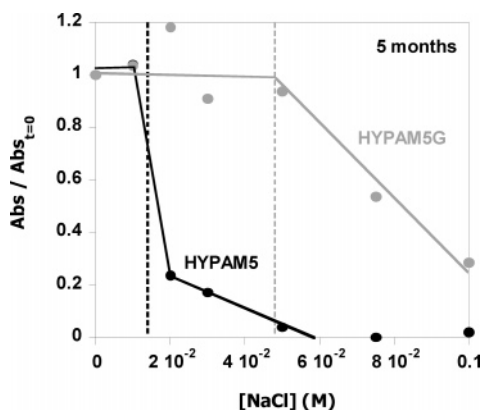


Figure 10. Evolution of absorbance at 520 nm as a function of the concentration of salt (NaCl) for gold nanoparticles stabilized by HYPAM5 (black circle) or HYPAM5G (gray circle).

aggregation (and precipitation) with time was followed by monitoring the decrease of the absorbance at 520 nm. The relative absorbance is reported in Figure 10 after 5 months as a function of NaCl concentrations for all solutions. The HYPAM5 stabilized nanoparticles were very sensitive to ionic strength even for low concentrations of NaCl. All solutions were completely sedimented after 1 week (for concentrations superior to 10^{-2} mol L⁻¹). In contrast, the functionalization of HYPAM5 by a gluconolactone shell completely prevented the aggregation promotion by salts in aqueous solutions. HYPAM5G stabilized gold nanoparticles solutions remained stable for weeks using salt concentrations up to 0.15 mol L⁻¹ and for months using salt concentrations up to $6 \cdot 10^{-2}$ mol L⁻¹ (Figure 10).

Conclusion

We synthesized, in a single step reaction, a new family of hyperbranched polymers HYPAM, which are chemically analogous to PAMAM dendrimers. Moreover, the molecular weight of the polymers was easily adjusted by changing the condition of reaction. HYPAMx were then used to prepare water stable gold nanoparticles. The open architecture of the HYPAM hyperbranched polymers facilitates the interactions between metal ions and polymer functional groups. Nevertheless, it maintains a control on the gold nanoparticles formed after reduction by sodium borohydride. Nanoparticles of ca. 4 nm were indeed obtained and stabilized in solution by the hyperbranched polymer. The average size of the nanoparticles could be easily adjusted by changing the [HAuCl₄]/[polymer] or [NaBH₄]/[HAuCl₄] ratios. The stability of the nanoparticles in water was mainly influenced by the molecular weight of the polymer core and the pH of the solutions. HYPAM functionalized by gluconolactone influences rather the stability of the nanoparticles than their size. Indeed, the presence of gluconolactone prevents the aggregation promotion by salts in aqueous solution. Experiments are also underway to use these polymer to stabilize platinum nanoparticles and to use them as water-soluble catalysts.

Acknowledgment. Authors wish to thank the NMR service of the Federation of Molecular Chemistry of Toulouse for quantitative ¹³C, COSY, HSQC and HMBC experiments, Y. Coppel from LCC (Toulouse) for quantitative ¹⁵N NMR measurements, and B. Payré and I. Fourquaux from CMEAB (Toulouse) for TEM measurements. The authors are indebted to M. Borkovec and D. Cakara for amine groups titration and helpful discussions.

Supporting Information Available: Experimental section consisting of figures showing NMR, complexation studies and TEM micrographs and text describing the experiments. This material is available free of charge via the Internet at <http://pubs.acs.org>.

References and Notes

- Bradley, J. S. *Clusters and Colloids, from Theory to Applications*; VCH: Weinheim, Germany, 1994.
- Taton, T. A.; Mirkin, C. A.; Letsinger, R. L. *Science* **2000**, *289*, 1757–1760.
- Turkevich, G.; Hillier, J.; Stevenson, P. C. *Discuss. Faraday Soc.* **1951**, *11*, 55–75.
- Sidorov, S. N.; Bronstein, L. M.; Valetsky, P. M.; Hartmann, J.; Cölfen, H.; Schnablegger, H.; Antonietti, M. *J. Colloid Interface Sci.* **1999**, *212*, 197–211.
- Bronstein, L. M.; Sidorov, S. N.; Gourkova, A. Y.; Valetsky, P. M.; Hartmann, J.; Breulmann, M.; Cölfen, H.; Antonietti, M. *Inorg. Chim. Acta* **1998**, *280*, 348–354.
- Zhou, Y.; Wang, C. Y.; Zhu, Y. R.; Chen, Z. Y. *Chem. Mater.* **1999**, *11*, 2310–2312.
- Mandal, M.; Ghosh, S. K.; Kundu, S.; Esumi, K.; Pal, T. *Langmuir* **2002**, *18*, 7792–7797.
- Zheng, P.; Jiung, X.; Zhang, X.; Zhang, W.; Shi, L. *Langmuir* **2006**, *22*, 9393–9396.
- Chen, S.; Guo, C.; Hu, G. H.; Wang, J.; Ma, J. H.; Liang, X. F.; Zheng, L.; Liu, H. Z. *Langmuir* **2006**, *22*, 9704–9711.
- Sakai, T.; Alexandridis, P. *Langmuir* **2005**, *21*, 8019–8025.
- Balogh, L.; Tomalia, D. A. *J. Am. Chem. Soc.* **1998**, *120*, 7355–7356.
- Zhao, M.; Sun, L.; Crooks, R. M. *J. Am. Chem. Soc.* **1998**, *120*, 4877–4878.
- Esumi, K.; Suzuki, A.; Aihara, N.; Usui, K.; Torigoe, K. *Langmuir* **1998**, *14*, 3157–3159.
- (a) Crooks, R. M.; Zhao, M.; Sun, L.; Chechik, V.; Yeung, L. K. *Acc. Chem. Res.* **2001**, *34*, 181–190. (b) Sun, X. P.; Dong, S. J.; Wang, E. K. *Macromolecules* **2004**, *37*, 7105–7108.
- Frechet, J. M. J.; Henmi, M.; Gitsov, I.; Aoshima, S.; Leduc, M. R.; Grubbs, R. B. *Science* **1995**, *269*, 1080–1082.
- Lu, Y.; Mei, Y.; Walker, R.; Ballauf, M.; Drechsler, M. *Polymer* **2006**, *47*, 4985–4995.
- Schlotterbeck, U.; Aymonier, C.; Thomann, R.; Hofmeister, H.; Tromp, M.; Richter, W.; Mecking, S. *Adv. Funct. Mater.* **2004**, *14*, 999–1004.
- Haag, R.; Krämer, M.; Stumbé, J.-F.; Krause, S.; Komp, A.; Prokhorova, S. *Polym. Prepr.* **2002**, *43*, 328.
- Mecking, S.; Thomann, R.; Frey, H.; Sunder, A. *Macromolecules* **2000**, *33*, 3958–3960.
- Tabuani, D.; Monticelli, O.; Chincarini, A.; Bianchini, C.; Vizza, F.; Moneti, S.; Russo, S. *Macromolecules* **2003**, *36*, 4294–4301.
- Garcia-Bernabé, A.; Krämer, M.; Oláh, B.; Haag, R. *Chem.—Eur. J.* **2004**, *10*, 2822–2830.
- Monticelli, O.; Russo, S.; Campagna, R.; Voit, B. *Polymer* **2005**, *46*, 3597–3606.
- Krämer, M.; Pérignon, N.; Haag, R.; Marty, J. D.; Thomann, R.; Lauth-de Viguerie, N.; Mingotaud, C. *Macromolecules* **2005**, *38*, 8308–8315.
- Pérignon, N.; Mingotaud, A.-F.; Marty, J.-D.; Rico-Lattes, I.; Mingotaud, C. *Chem. Mater.* **2004**, *16*, 4856–4858.
- Dvornic, P. R.; Hu, J.; Meier, D. J.; Nowak, R. M.; Parham, P. L. US Patent, 2002.
- Dvornic, P. R.; Li, J.; de Leuze-Jallouli, A. M.; Reeves, S. D.; Owen, M. J. *Macromolecules* **2002**, *35*, 9323–9333.
- Zeng, F.; Shen, Y.; Zhu, S.; Pelton, R. *Macromolecules* **2000**, *33*, 1628.
- Zagar, E.; Zigon, M. *Macromolecules* **2002**, *35*, 9913–9925.
- Schmitzer, A. R.; Franceschi, S.; Perez, E.; Rico-Lattes, I.; Lattes, A.; Thion, L.; Erard, M.; Vidal, C. *J. Am. Chem. Soc.* **2001**, *123*, 5956–5961.
- Hong, L.; Wang, X.; Tang, X. *J. Appl. Polym. Sci.* **2002**, *85*, 2445–2450.
- Podzimek, S.; Vlcek, T.; Johann, C. *J. Appl. Polym. Sci.* **2001**, *81*, 1588–1594.
- Kunamaneni, S.; Buzza, D. M.; Parker, D.; Feast, W. J. *J. Mater. Chem.* **2003**, *13*, 2749–2755.
- Cakara, D.; Kleimann, J.; Borkovec, M. *Macromolecules* **2003**, *36*, 4201–4207.
- Koper, G. J. M.; van Genderen, M. H. P.; Elissen-Roman, C.; Baars, M. W. P. L.; Meijer, E. W.; Borkovec, M. *J. Am. Chem. Soc.* **1997**, *119*, 6512–6521.
- Niu, Y.; Sun, L.; Crooks, R. M. *Macromolecules* **2003**, *36*, 5725–5731.

- (36) Hobson, L. J.; Feast, W. J. *Polymer* **1999**, *40*, 1279–1297.
- (37) Ottaviani, M. F.; Montaldi, F.; Turro, N. J.; Tomalia, D. A. *J. Phys. Chem. B* **1997**, *101*, 158–166.
- (38) Scott, R. W. J.; Wilson, O. M.; Crooks, R. M. *J. Phys. Chem. B* **2005**, *109*, 692–704.
- (39) Yonezawa, Y.; Kawabata, I.; Sato, T. *Bunsen-Ges. Phys. Chem.* **1996**, *100*, 39–45.
- (40) Esumi, K.; Hosoya, T.; Suzuki, A.; Torigoe, K. *J. Colloid Interface Sci.* **2000**, *226*, 346–352.
- (41) Esumi, K.; Kameo, A.; Suzuki, A.; Torigoe, K. *Colloids Surf. A: Physiochem. Eng. Aspects* **2001**, *189*, 155–161.
- (42) Esumi, K.; Torigoe, K. *Prog. Colloid Polym. Sci.* **2001**, *117*, 80–87.
- (43) Zheng, J.; Stevenson, M. S.; Hikida, R. S.; van Patten, P. G. *J. Phys. Chem. B* **2002**, *106*, 1252–1255.

MA070176M